Condensation transition in the one-dimensional extended Hubbard model

H. Q. Lin and J. E. Hirsch
Department of Physics, University of California, San Diego, La Jolla, California 92093
(Received 3 September 1985)

We study the phase diagram of the one-dimensional extended Hubbard model in the half-filled-band sector for an attractive nearest-neighbor interaction V. A first-order condensation transition occurs at a critical value of V which is a function of the on-site repulsion U. We obtain the phase boundary in strong coupling for $U\to\infty$ and $U\to-\infty$, and, from a variational estimate, for $U=0$. We then compute the phase boundary numerically using a Monte Carlo simulation technique. Our numerical estimates join smoothly the strong-coupling regimes for $|U|\sim 4$, and agree with the variational estimate at $U=0$ within 10%.

I. INTRODUCTION

The phase diagram of the one-dimensional electron gas has been extensively studied in recent years, using a variety of analytic techniques[1,2] and more recently Monte Carlo simulation methods.[3,4] While the analytic approaches usually define the model by specifying the couplings in momentum space, for the numerical approaches it is more convenient to define the model in real space. In addition, the interaction parameters in real space have a more direct interpretation in terms of overlap matrix elements of molecular orbitals in a tight-binding picture. The simplest model defined in real space that can be put in one-to-one correspondence with the electron-gas model is the extended Hubbard model with on-site interaction U and nearest-neighbor interaction V.[2] One would also expect these interactions to be the dominant ones in a quasi-one-dimensional narrow-band material for which the model might be appropriate, both because of exponential decay of overlap matrix elements and because of screening. Since the electron-electron interaction parameters U and V will, in general, be a combination of direct Coulomb repulsion and indirect attraction mediated by phonons or excitons (neglecting retardation), it is of interest to study the phase diagram of the model for both positive and negative values of U and V.

In the half-filled-band sector, there are two regimes of the extended Hubbard model which one expects will have long-range order. For sufficiently large repulsive V, the model will undergo a transition to a charge-density-wave (CDW) state of period 2 in real space. For sufficiently large attractive V, Haldane[5] has recently predicted the existence of a condensation transition line. For repulsive V the phase boundary has recently been studied in detail using Monte Carlo simulations,[4] and the purpose of this paper is to study the phase boundary for attractive V. Within these two boundary lines the system still exhibits a rich structure characterized by algebraic decay of various correlation functions which has been studied in weak coupling using renormalization-group techniques. Numerical studies of that region will be reported in the future.

The model is defined by the Hamiltonian

$$H=-t\sum_{i=1,\sigma=\uparrow\downarrow}^{N}(C_{i\sigma}^{\dagger}C_{i+1,\sigma}+\text{H.c.})+U\sum_{i=1}^{N}n_{i\uparrow}n_{i\downarrow}+V\sum_{i=1}^{N}n_i n_{i+1}\,, \tag{1.1}$$

where $n_{i\sigma}=C_{i\sigma}^{\dagger}C_{i\sigma}$ And $n_i=n_{i\uparrow}+n_{i\downarrow}$.

We will define our energy units by setting $t=1$ in what follows, and we restrict ourselves to the half-filled-band sector (one electron per site). In the next section we discuss the condensation transition in the limits $U\to\infty$ and $U\to-\infty$, and a variational estimate for the transition point at $U=0$. In Sec. III we briefly discuss the simulation method used and the methods we have used to determine the phase boundary from our simulation results. We present numerical results in Sec. IV and summarize our conclusions in Sec. V.

II. SOME LIMITING CASES

A. $U, |V| \gg 1$

If we neglect the hopping, the Hamiltonian can be written as

$$H=\sum_{i=1}^{N}H(i)\,, \tag{2.1a}$$

where

$$H(i)=Un_{i\uparrow}n_{i\downarrow}+Vn_i n_{i+1}=\left[\frac{U}{2}+2V\right]n_i-\left[\frac{U}{2}+V\right](n_{i\uparrow}-n_{i\downarrow})^2-\frac{V}{2}(n_i-n_{i+1})^2 \tag{2.1b}$$

and the energy

$$E=\langle H\rangle=H\,,$$

with n_i being a c number now. Since $V<0$, the ground state for $U+2V>0$ has only singly occupied sites:

$$n_{i+1}=n_i;\ \ n_{i\uparrow}=1,\ n_{i\downarrow}=0 \ \text{ or } \ n_{i\uparrow}=0,\ n_{i\downarrow}=1 \tag{2.2a}$$

with energy

$$E=NV\ . \tag{2.2b}$$

This state is highly degenerate, since the energy is independent of the spin orientation at each site.

For $U+2V<0$, the energy will be most negative if

$$n_{i+1}=n_i \ \text{ and } n_{i\uparrow}=n_{i\downarrow} \tag{2.3a}$$

with energy

$$E=N\frac{U}{2}+\left[\frac{N}{2}-1\right]4V\ . \tag{2.3b}$$

This is a condensed state, where all sites are doubly occupied in half the system, and the other half is empty. So the transition line for $t=0$ is $U=-2V$ as $N\to\infty$.

When hopping is included, the correction to the ground-state energy of the condensed state in second-order perturbation theory is $t^2/(-U-V)$. This correction is of order 1. The correction to the state with singly occupied sites is, however, of order N because of the high degeneracy. In second-order perturbation theory one obtains an effective Hamiltonian describing a Heisenberg antiferromagnet with coupling:

$$J_{\text{eff}}=\frac{t^2}{U-V}\ ,$$

so that the ground state will have long-range antiferromagnetic correlations, i.e., a spin-density-wave (SDW) state. The ground-state energy is, using the Bethe-ansatz result,

$$E=N\left[V-\frac{4t^2\ln 2}{U-V}\right]\ . \tag{2.4}$$

Equating the energies of the condensed and SDW states we get the phase boundary for large U and V as $N\to\infty$:

$$V=-\frac{U}{2}-\frac{8t^2\ln 2}{3U}\ . \tag{2.5}$$

B. $U,V<0\,|U|>>1,\,|V|$

As shown by Emery,[6] the effective Hamiltonian to second order in the hopping and first order in V is again an antiferromagnetic Heisenberg model:

$$H_{\text{eff}}=-\sum_{i=1}^{N}\left(J_xS_{i,x}S_{i+1,x}+J_yS_{i,y}S_{i+1,y}+J_zS_{i,z}S_{i+1,z}\right) \tag{2.6a}$$

with

$$J_x=J_y=\frac{4t^2}{|U|}\ ,\qquad J_z=-J_x-4V\ , \tag{2.6b}$$

and

$$S_i^+=C_{i\downarrow}^\dagger C_{i\uparrow}^\dagger\ ,\qquad S_i^-=C_{i\uparrow}C_{i\downarrow}\ ,\qquad S_{i,z}=(n_{i\uparrow}+n_{i\downarrow}-1)/2\ , \tag{2.6c}$$

i.e., spin up corresponds to doubly occupied sites and spin down to empty sites.

When $J_z=J_x$ there is a first-order transition to a ferromagnetic state. In the Heisenberg model, this corresponds to half of the system having spin up and half spin down, since the total magnetization is conserved. In the Hubbard model, it corresponds to the condensation transition. Hence, the transition line in this limit is given by

$$V=-\frac{2t^2}{|U|}\ . \tag{2.7}$$

C. $U=0$

If $V=0$, the kinetic part of the Hamiltonian can be diagonalized and the eigenvalues are

$$e_k=-2t\cos\left[\frac{2\pi k}{N}\right],\ k=0,1,\ldots,N-1\ .$$

Let us take this free-electron-gas wave function as our trial wave function and calculate the expectation value of the Hamiltonian $\langle H\rangle$ with this wave function. We have then, for the half-filled band:

$$E_{\text{var}}=\langle H\rangle=-4t\sum_{k=-N/4}^{N/4-1}\cos\left[\frac{2\pi k}{N}\right]+V\sum_{i=1}^{N}\langle n_in_{i+1}\rangle$$

$$=-4t\frac{\cos(\pi/N)}{\sin(\pi/N)}+NV\left[1-\frac{2}{N^2}\left[\frac{\cos(\pi/N)}{\sin(\pi/N)}\right]^2\right]\sim N\left[-\frac{4t}{\pi}+V\left[1-\frac{2}{\pi^2}\right]\right]\ \text{ as } N\to\infty\ . \tag{2.8}$$

On the other hand, the expectation value of the Hamiltonian in the perfectly condensed state is

$$E=4V\left[\frac{N}{2}-1\right]=2VN-4V\ . \tag{2.9}$$

As a crude estimation, we equate these two energies and let $N\to\infty$:

$$2V=-\frac{4t}{\pi}+V\left[1-\frac{2}{\pi^2}\right], \tag{2.10a}$$

i.e.,

$$V=-\frac{4t}{\pi+2/\pi}=-1.0587\ . \tag{2.10b}$$

So the system will not condense for $V>-1.0587$, and we expect the actual transition value of V to be somewhat lower than this. The reason is that for such a large value of V the ground state in the noncondensed phase will probably be quite different from that of our free-electron variational state, giving a lower energy. On the other hand, the true ground state in the condensed phase is probably not very far from our variational estimate.

III. METHODS TO DETERMINE THE PHASE BOUNDARY

Having seen the qualitative and quantitative behaviors in limiting cases, we turn our attention to intermediate values of U. The weak-coupling renormalization-group calculations predict that the system will have algebraic SDW order for $U>2V$, $U>-2V$ and long-range CDW order for $U<2V$, $V>0$, while singlet superconducting (SS) pairing dominates in the region $U<2V<0$, and triplet superconducting pairing dominates in the region $-2V>U>2V$. We have seen that in strong coupling a condensed phase should exist for both $U\to\infty$ and $U\to-\infty$, so that one may expect a continuous phase boundary separating the condensed phase from the other phases as a function of U. In order to determine the location of this phase boundary, we use the Monte Carlo (MC) simulation method described in Ref. 7, which treats the system in the canonical ensemble (fixed total number of electrons). In the following we discuss the methods we used to determine this phase boundary.

A. $S(Q_{\min})$

An appropriate quantity to determine the condensed phase is the Fourier transform of the electron-density correlation function at wave vector $q=Q_{\min}=2\pi/N$, defined by

$$D(l)=\frac{1}{N}\sum_{i=1}^{N}(\langle n_i n_{i+1}\rangle-\langle n_i\rangle\langle n_{i+1}\rangle) \tag{3.1a}$$

and its Fourier transform, the so-called structure factor

$$S(q)=\sum_{l=0}^{N-1}D(l)e^{iql},\quad q=\frac{2\pi}{N}\times(0,\ldots,N-1)\ . \tag{3.1b}$$

In the perfect charge-density-wave (CDW) phase $n_i=(-1)^i+1$, so that

$$\begin{aligned}&D(2j+1)=-1\ ,\\ &D(2j)=1,\quad j=0,1,\ldots,N/2-1\end{aligned} \tag{3.2a}$$

and

$$\begin{aligned}&S(\pi)=N\ ,\\ &S(q)=0\ \text{ for } all\ q\neq\pi\ ,\end{aligned} \tag{3.2b}$$

while in the perfect condensed phase, $n_i=2(0)$ for $i<N/2$ ($>N/2$), and we have

$$D(j)=-D\left[\frac{N}{4}+j\right]=1-4\frac{j}{N},\quad j=0,1,\ldots,N/2 \tag{3.3a}$$

and then

$$S(q)=2\frac{1-(-1)^k}{N\sin^2(q/2)},\quad k=q/Q_{\min}\ . \tag{3.3b}$$

The largest one is that with $q=2\pi/N$, in which

$$S(Q_{\min})=S\left[\frac{2\pi}{N}\right]\to\frac{4N}{\pi^2}\ \text{ as } N\to\infty\ .$$

The zero-frequency SDW susceptibility is defined by

$$\chi_{\mathrm{SDW}}(q)=\frac{1}{N}\int_0^\beta d\tau\sum_{i,j}\langle[n_{i\uparrow}(\tau)-n_{i\downarrow}(\tau)][n_{i\uparrow}(0)-n_{i\downarrow}(0)]\rangle e^{iq|\mathbf{R}_i-\mathbf{R}_j|},\quad q=\frac{2\pi}{N}\times(0,\ldots,N-1)\ .$$

$\chi_{\mathrm{SDW}}(q=\pi)$ should diverge in the SDW phase but is very small in both the condensed and CDW phases.

B. Histogram

To help determine whether we have a condensed phase, we look at histograms of the occupation number. Since the total particle number is fixed in the canonical ensemble, we measure particle number in certain number of adjacent sites instead of over the whole lattice. Let N be the lattice size, and M the size of our measuring "window." We sweep with this window across the entire lattice, and measure $p(n)$, the number of times the occupation number in our window is nM ($0\le n\le 2$). It is easy to see that if we are in a phase where all sites are singly occupied, or in the perfectly ordered CDW phase, then $p(1)=N$ (for $M>1$) and $p(n)=0$ for $n\neq 1$, while in the perfectly condensed phase $p(n)$ will be nonzero for $n=0$ and 2, provid-

ed $M \leq N/2$. To get a clear indication of the condensed state we found it most convenient to take $M=N/4$. In that case, $p(n)$ is sharply peaked around $n=0$ and 2 in the perfectly condensed state and we expect this qualitative feature to persist in the presence of fluctuations. In contrast, in the noncondensed phase $p(n)$ will always be peaked around $n=1$.

C. Problems at large U

There are some problems that we should pay special attention in doing MC simulations when we are in large-U region. The transition is strongly first order there and the energy barrier between the two phases is very large, making it very difficult for the system to reach equilibrium. If the simulations were started on the "wrong side" of the phase boundary, the system could stay there very long before going into the "right side" of phase boundary. To overcome this difficulty we start the simulations in the SDW phase, in the condensed phase, and in a mixed phase with one-half of the lattice in the condensed phase and one-half in the SDW phase. After several hundred sweeps we measure the energy in each phase. By comparing the energies we can determine the transition point to the required accuracy. The mixed phase usually (but not always) converges to the phase of lower energy, so that this is an alternative way to determine the phase transition point.

Another problem to be noted here is the effect of size dependence which is especially important in doing MC simulations because we always deal with finite lattices. Such effect in determining the transition point V is, as a crude estimate from Eq. (2.3b), $\Delta V = V - V(N) \approx -4V/N$. Though the hopping term might compensate this for small U, it cannot be neglected for large U since there $V \approx -U/2$. Thus, it is essential to extrapolate the size dependence, particularly for strong coupling. We plot $V(N)$ versus $1/N$ for different lattice size N and extrapolate it to $N \to \infty$. This procedure is found to work very well in our simulations.

IV. SIMULATION RESULTS

In this section we discuss our simulation results of the extended Hubbard model in the region $V<0$. The Monte Carlo simulation method used is described in detail in Ref. 7, and other studies of the Hubbard model in Refs. 3 and 4. We have performed our simulations on lattices of up to $N=32$ sites, with time-slice size $\Delta\tau=0.25$ and number of time slices $L=N$. Typical simulations involved 20 000 sweeps through the lattice and doing measurements every 5 or 10 sweeps depending on the acceptance of the move. The system takes a very long time to equilibrate, especially for large lattices and strong couplings. To make sure that we were getting correct statistical averages we repeated the simulations several times with different initial random number seed to see if the results were coincident within the errors. The simulations were performed on a Ridge 32 minicomputer.

We started our MC simulations for the case $U=0$. Figure 1 shows the structure factor $S(q)$ and Fig. 2 the zero-frequency SDW susceptibility $\chi_{\rm SDW}(q)$ versus q for $N=32$, $U=0$, and $V=-1.0$, -1.1, -1.15, and -1.2. $S(q)$ is small for all q for $V \geq -1.1$, and a peak at $q=Q_{\rm min}$ appears and grows rapidly as V is decreased. $\chi_{\rm SDW}(\pi)$ is rapidly suppressed as V decreases from -1.1 to -1.2. It is clear from these results that the system undergoes the condensation transition between $V=-1.15$ and -1.2. Histograms for $N=32$, $U=0$, and $V=-1.0$,

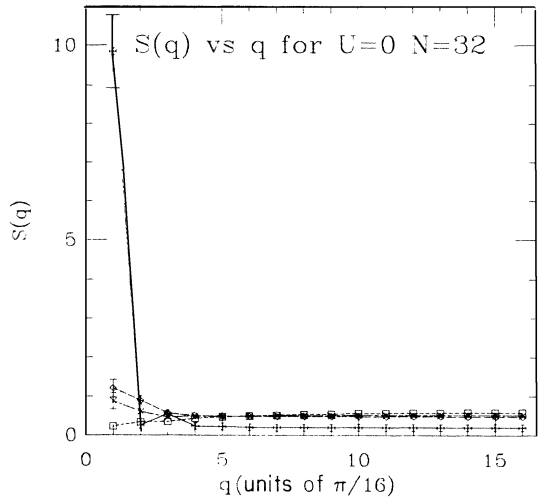

FIG. 1. Structure factor $S(q)$ for a 32-site ring at $U=0$ and $V=-1.0$ (dotted line and square), $V=-1.1$ (dotted-dashed line and cross), $V=-1.15$ (dashed line and diamond), and $V=-1.2$ (solid line and fancy diamond). The sudden jump at $q=Q_{\rm min}$ for $V=-1.2$ indicates that the transition is first order.

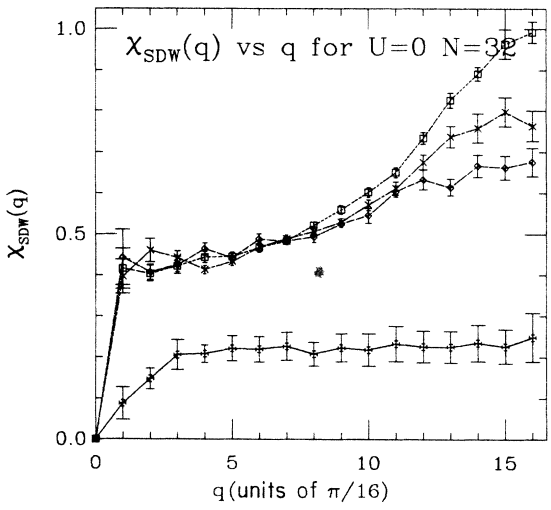

FIG. 2. Zero-frequency SDW susceptibility $\chi_{\rm SDW}(q)$ for a 32-site ring at $U=0$ and $V=-1.0$ (dotted line and square), $V=-1.1$ (dotted-dashed line and cross), $V=-1.15$ (dashed line and diamond), and $V=-1.2$ (solid line and fancy diamond).

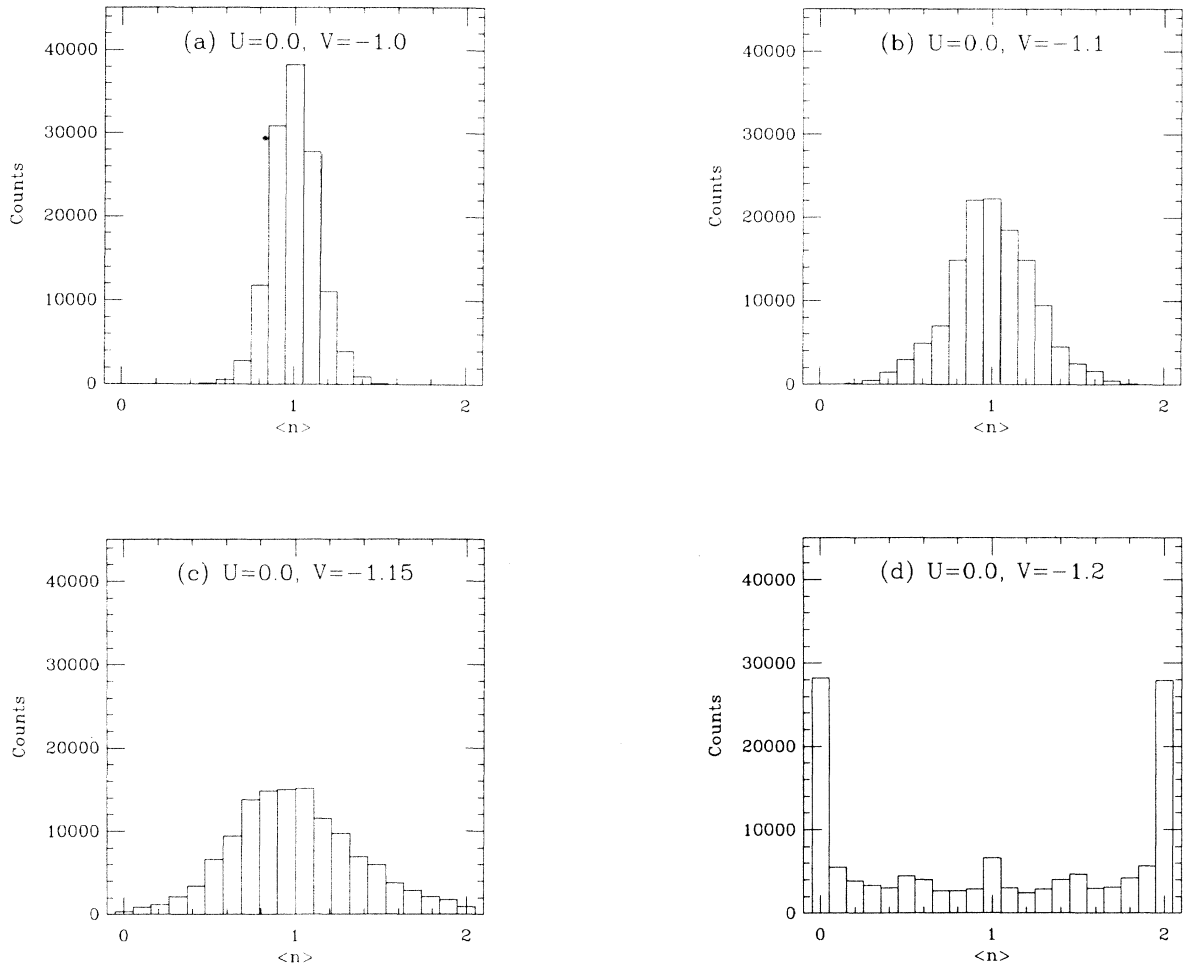

FIG. 3. Histograms of the occupation number of $N/4$ adjacent sites for a 32-site ring at $U=0$ and $V=-1.0$, -1.1, -1.15, and -1.2. The histogram is peaked around $n=1$ in the SDW phase and at $n=0$ and 2 in the condensed phase.

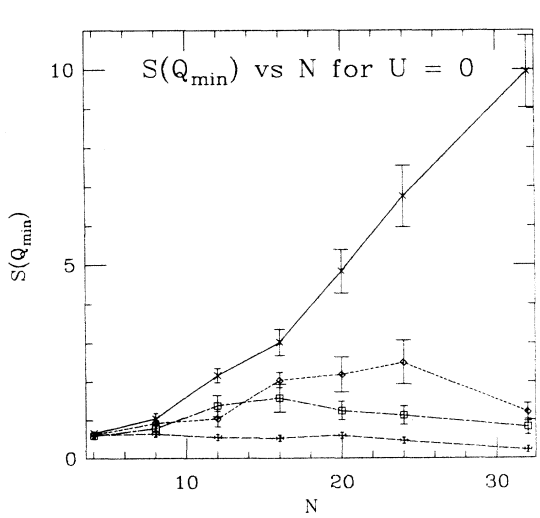

FIG. 4. Structure factor $S(Q_{\min})$ vs lattice size N for $U=0$ and $V=-1.0$ (dashed line and fancy diamond), $V=-1.1$ (dotted-dashed line and square), $V=-1.15$ (dotted line and diamond), and $V=-1.2$ (solid line and cross).

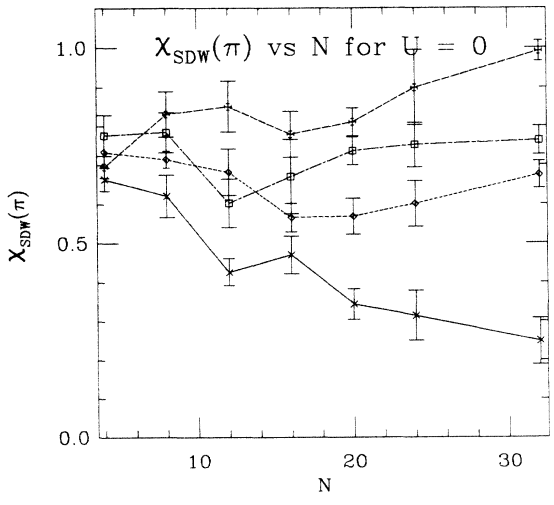

FIG. 5. Zero-frequency SDW susceptibility $\chi_{\mathrm{SDW}}(\pi)$ vs lattice size N for $U=0$ and $V=-1.0$ (dashed line and fancy diamond), $V=-1.1$ (dotted-dashed line and square), $V=-1.15$ (dotted line and diamond), and $V=-1.2$ (solid line and cross).

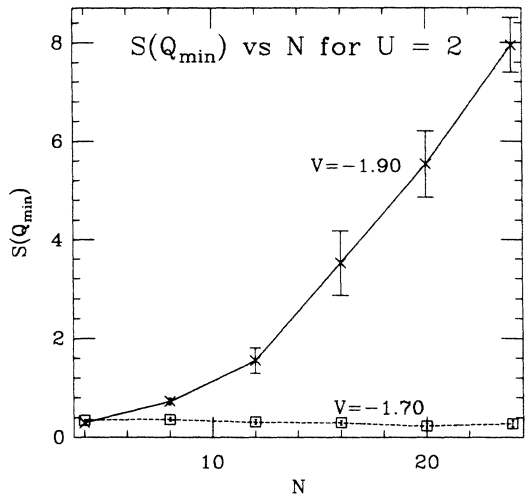

FIG. 6. Structure factor $S(Q_{\min})$ vs lattice size N for $U=2.0$ and $V=-1.70$ (dotted line and fancy diamond) and $V=-1.90$ (solid line and cross).

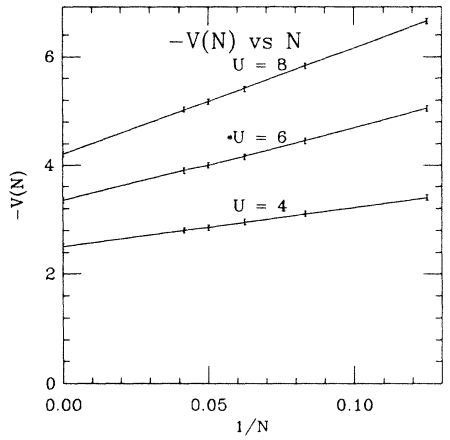

FIG. 8. Transition value V vs lattice size N for $U=4.0$, 6.0, and 8.0. The extrapolated transition value at $N=\infty$ is $V=-2.50\pm0.05$ for $U=4.0$, $V=-3.35\pm0.05$ for $U=6.0$, and $V=-4.20\pm0.05$ for $U=8.0$.

-1.1, -1.15, and -1.2 are shown in Fig. 3. For $V=-1.0$, Fig. 3 shows a narrow peak around $n=1$. As V decreases this peak broadens, and when the system condenses the histogram shows peaks at $n=0$ and 2, as expected.

If we scale the spatial size and the inverse temperature by the same factor, $S(Q_{\min})$ should diverge linearly with N in the condensed phase and $\chi_{SDW}(\pi)$ should diverge linearly in the SDW phase. Figures 4 and 5 show the results for $V=-1.0$, -1.1, -1.15, and -1.2. The results for $S(Q_{\min})$ indicate clearly that the transition point for $U=0$ is around $V=-1.15\pm0.05$. It is somewhat more negative than the value estimated in Sec. II C ($V=-1.0587$), as expected. The results for $\chi_{SDW}(\pi)$ show that these correlations become smaller as tempera-

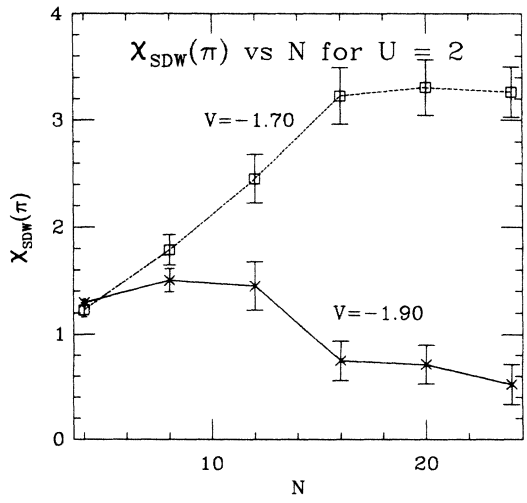

FIG. 7. Zero-frequency SDW susceptibility $\chi_{SDW}(\pi)$ vs lattice size N for $U=2.0$ and $V=-1.70$ (dotted line and fancy diamond) and $V=-1.90$ (solid line and cross).

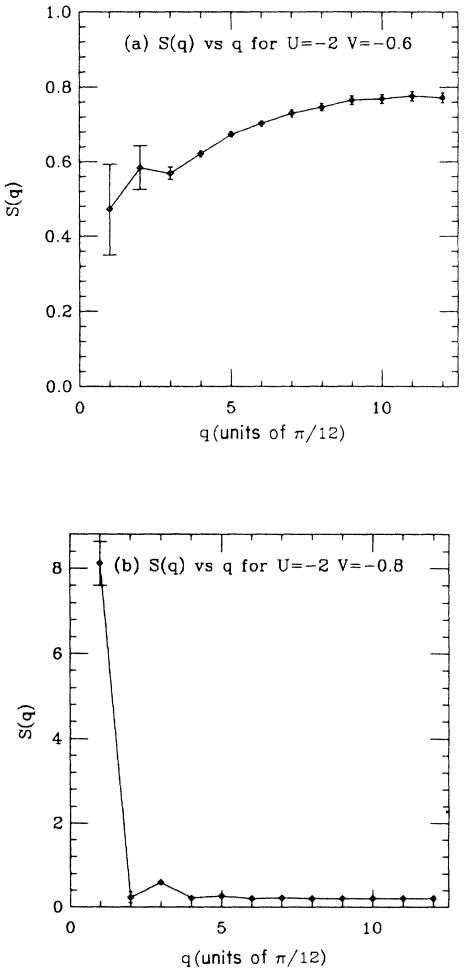

FIG. 9. Structure factor $S(q)$ for a 24-site ring at $U=-2.0$, (a) $V=-0.6$, where the maximum is at $q=\pi$, and (b) $V=-0.8$, where the maximum is at $q=Q_{\min}$.

TABLE I. $E(N,V)$ for $U=4.0$.

N	V	E(condensed)	E(SDW)	$V(N)$
8	−3.45	−3.862 (0.021)	−3.801 (0.014)	
	−3.35	−3.807 (0.013)	−3.816 (0.024)	
	−3.40	−3.883 (0.013)	−3.877 (0.016)	−3.40 (0.05)
12	−3.15	−3.684 (0.003)	−3.669 (0.018)	
	−3.05	−3.501 (0.015)	−3.582 (0.009)	
	−3.10	−3.584 (0.009)	−3.613 (0.011)	−3.11 (0.05)
16	−3.00	−3.591 (0.004)	−3.561 (0.005)	
	−2.90	−3.422 (0.005)	−3.463 (0.006)	−2.95 (0.05)
20	−2.90	−3.505 (0.001)	−3.473 (0.005)	
	−2.80	−3.336 (0.002)	−3.367 (0.004)	−2.85 (0.05)
24	−2.85	−3.468 (0.001)	−3.414 (0.007)	
	−2.75	−3.291 (0.001)	−3.331 (0.003)	
	−2.80	−3.380 (0.001)	−3.372 (0.004)	−2.80 (0.05)

TABLE III. $E(N,V)$ for $U=8.0$.

N	V	E(condensed)	E(SDW)	$V(N)$
8	−6.70	−7.165 (0.001)	−7.136 (0.033)	
	−6.60	−7.015 (0.0001)	−7.045 (0.021)	
	−6.65	−7.090 (0.001)	−7.089 (0.018)	−6.65 (0.05)
12	−5.90	−6.425 (0.003)	−6.392 (0.011)	
	−5.80	−6.270 (0.003)	−6.300 (0.030)	
	−5.85	−6.348 (0.002)	−6.356 (0.021)	−5.84 (0.05)
16	−5.45	−6.038 (0.001)	−5.980 (0.011)	
	−5.35	−5.872 (0.002)	−5.879 (0.011)	
	−5.40	−5.959 (0.002)	−5.966 (0.009)	−5.40 (0.05)
20	−5.20	−5.785 (0.001)	−5.769 (0.006)	
	−5.10	−5.616 (0.001)	−5.650 (0.008)	−5.17 (0.05)
24	−5.05	−5.626 (0.001)	−5.622 (0.008)	
	−5.00	−5.539 (0.001)	−5.576 (0.006)	−5.03 (0.05)

ture is reduced in the condensed phase. In the noncondensed phase, these correlations do not appear to diverge, in agreement with the renormalization-group predictions.

In the same manner we performed Monte Carlo simulations at $U=2.0$, and some results are shown in Figs. 6 and 7. The transition point is $V=-1.80\pm0.10$.

As we mentioned before, it is important to pay attention to the size dependence and large energy barrier for large values of U. For $U=4$, 6, and 8, 4000 to 15 000 MC iterations were run before measuring the energies. The pictures of electron configurations after warm-up helped us to determine what phase of the system we were measuring. Typically 1000 measurements were made separated by 5 ($U=4$) and 10 ($U=6,8$) MC runs. Table I lists the results for $U=4$ at $N=8$, 12, 16, 20, and 24, Table II for $U=6$, and Table III for $U=8$. From these results we estimated the transition points $V(N)$ and plot them versus $1/N$ in Fig. 8. The results fit a linear dependence well, and the transition values for V for the infinite system deduced by extrapolation are $V=-2.50\pm0.05$ for $U=4$, $V=-3.35\pm0.05$ for $U=6$, and $V=-4.20\pm0.05$ for $U=8$. Note how the size dependence becomes stronger as U increases. The transition values obtained from the strong-coupling perturbation calculation, Eq. (2.5), are $V=-2.4621$ for $U=4$, $V=-3.3081$ for $U=6$, and $V=-4.2310$ for $U=8$. So we already join the strong-coupling results at $U=4$ and beyond. This is in contrast with the results obtained for the CDW transition, where even for $U=8$ the MC results were somewhat smaller than the strong-coupling predictions.

We next consider the negative-U region. According to the renormalization-group predictions, SS correlations should diverge for $U<2V$. Unfortunately, our MC pro-

TABLE II. $E(N,V)$ for $U=6.0$.

N	V	E(condensed)	E(SDW)	$V(N)$
8	−5.10	−5.514 (0.001)	−5.509 (0.027)	
	−5.00	−5.364 (0.001)	−5.413 (0.022)	
	−5.05	−5.439 (0.001)	−5.464 (0.022)	−5.05 (0.05)
12	−4.50	−5.012 (0.003)	−4.993 (0.013)	
	−4.40	−4.857 (0.002)	−4.883 (0.008)	
	−4.45	−4.932 (0.002)	−4.909 (0.023)	−4.45 (0.05)
16	−4.20	−4.771 (0.001)	−4.740 (0.007)	
	−4.10	−4.604 (0.002)	−4.609 (0.010)	
	−4.15	−4.690 (0.001)	−4.690 (0.012)	−4.15 (0.05)
20	−4.05	−4.644 (0.001)	−4.574 (0.017)	
	−3.95	−4.472 (0.001)	−4.503 (0.005)	
	−4.00	−4.557 (0.001)	−4.562 (0.006)	−4.00 (0.05)
24	−3.95	−4.545 (0.001)	−4.513 (0.004)	
	−3.85	−4.368 (0.001)	−4.416 (0.006)	−3.89 (0.05)

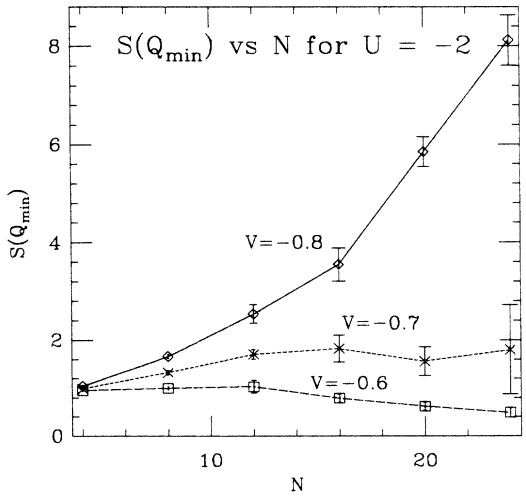

FIG. 10. Structure factor $S(Q_{\min})$ vs lattice size N for $U=-2.0$ and $V=-0.6$ (dashed line and fancy diamond), $V=-0.7$ (dotted line and cross), and $V=-0.8$ (solid line and diamond).

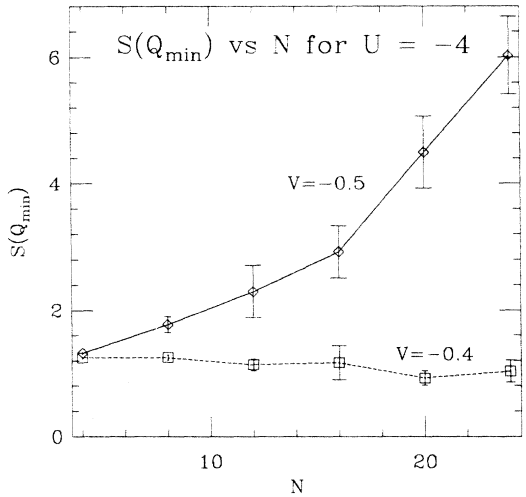

FIG. 11. Structure factor $S(Q_{\min})$ vs lattice size N for $U=-4.0$ and $V=-0.4$ (dotted line and square) and $V=-0.5$ (solid line and diamond).

gram does not measure SS correlations. For small negative V, CDW correlations, i.e., $S(q=\pi)$, should also diverge for $U<0$, but not when we approach the condensation point. $S(Q_{\min})$ still will diverge as the system approaches the condensed phase. Figure 9(a) shows the structure factor $S(q)$ versus q for the 24-site ring at $U=-2$, $V=-0.6$, where we see increasing of $S(q)$ with increasing q. The maximum is at $q=\pi$. Opposite behavior occurs for $V=-0.8$, where the maximum is at $q=Q_{\min}$ [Fig. 9(b)]. We plot $S(Q_{\min})$ versus lattice size N in Fig. 10 for $V=-0.6$, -0.7, and -0.8. It clearly indicates that the system is in the condensed phase when $V=-0.8$ and the transition point is $V=-0.7\pm0.1$. Proceeding in the same way for $U=-4$, $V=-0.4$, and $V=-0.5$, we present the results of $S(Q_{\min})$ versus N in Fig. 11. The transition point is $U=-4.0$, $V=-0.45\pm0.05$. This is close to the value $V=-0.5$ as calculated from Eq. (2.7) by strong-coupling perturbation theory.

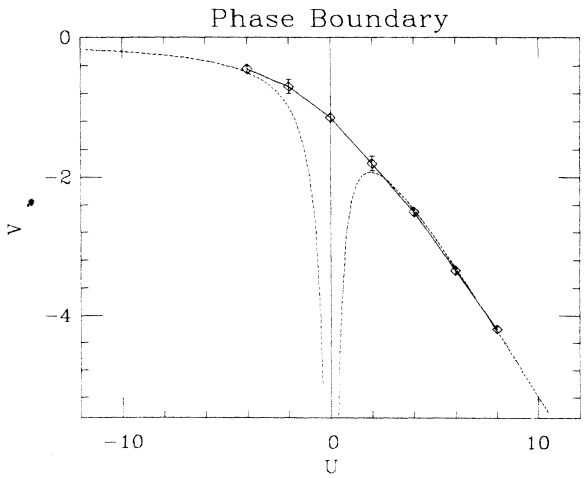

FIG. 12. Phase boundary of the condensation region. The solid line connects the Monte Carlo results (diamonds) and the two dotted lines are the strong-coupling predictions for $U\to\infty$ and $U\to-\infty$, respectively.

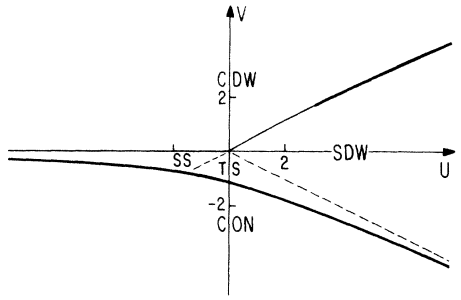

FIG. 13. Phase diagram of the one-dimensional half-filled extended Hubbard model. The thick lines indicate first-order transitions. CON denotes the condensed phase.

Considering the error in our estimation $\Delta V=0.05$, we conclude that it starts to merge with the line given by Eq. (2.7) beyond $U=-4.0$.

To summarize, we show the phase boundary in Fig. 12. The two limiting cases for large $|U|$ are shown as dotted lines and the Monte Carlo–simulation results are shown as the points connected by the solid line. The transition is first order everywhere along that line, in contrast with the CDW-SDW transition, which becomes continuous for small values of U.

V. SUMMARY

We have studied the phase boundary where the electrons undergo a condensation transition in the one-dimensional extended Hubbard model with attractive interactions between nearest-neighbor sites. From perturbation theory we found that a condensation transition should occur both for large positive and negative U for sufficiently large negative V, and Monte Carlo simulations allowed us to conclude that there exists a continuous phase boundary connecting both strong-coupling solutions. The strong-coupling predictions for the phase boundary were found to be quite accurate for $|U|\geq4$. To summarize, our present knowledge of the phase diagram of the one-dimensional half-filled extended Hubbard model is shown in Fig. 13. The line $V=0$, $U<0$ for the CDW-SS phase boundary can be obtained by symmetry arguments, and the other solid lines in the diagram were obtained by Monte Carlo simulations in previous work[4] and in the present work. The dashed lines in the diagram are renormalization-group predictions[1,2] which are probably accurate but have been tested numerically only qualitatively to date.[7]

ACKNOWLEDGMENTS

We are grateful to Dr. D. Haldane for sharing his insights on this problem with us. This work was partially supported by the National Science Foundation under Grant No. DMR-82-17881. In addition, one of us (H.Q.L.) is grateful to the Exxon Education Foundation and the other of us (J.E.H.) is grateful to the Sloan Foundation for financial support.

[1]J. Solyom, Adv. Phys. **21**, 201 (1979).
[2]V. J. Emery, in *Highly Conducting One-Dimensional Solids,* edited by J. Devreese, R. Evrand, and V. van Doren (Plenum, New York, 1979).
[3]J. E. Hirsch and D. J. Scalapino, Phys. Rev. B **27**, 7169 (1983); **29**, 5554 (1984).
[4]J. E. Hirsch, Phys. Rev. Lett. **53**, 2327 (1984).
[5]D. Haldane (private communication).
[6]V. J. Emery, Phys. Rev. B **14**, 2989 (1976); see also M. Fowler, *ibid.* **17**, 2989 (1978).
[7]J. E. Hirsch, D. J. Scalapino, R. L. Sugar, and R. Blankenbecler, Phys. Rev. B **26**, 5033 (1982).